TECHNICAL MEMORANDUM

173

Momentum budgets

E. Klinker

Research Department

August 1990 (SAC Paper)

European Centre for Medium-Range Weather Forecasts
Europäisches Zentrum für mittelfristige Wettervorhersage
Centre européen pour les prévisions météorologiques à moyen

E.C.M.W.F.
SCIENTIFIC ADVISORY COMMITTEE
18th SESSION

ECMWF/SAC(90)5
SHINFIELD
16 August 1990

MOMENTUM BUDGETS

1. INTRODUCTION

The last major model change in May 1989 had a pronounced impact on the parametrized thermal and mechanical forcing of the atmosphere. With the new radiation scheme the model produced larger long wave radiative cooling rates in the mid-troposphere and in the stratosphere. The replacement of the old convection scheme by the mass flux approach had important implications for the meridional circulation: the increased diabatic heating rates in cumulus convection enhanced the Hadley circulation and extended it to higher levels.

In addition to the indirect influence of the thermal forcing on momentum, changes in the parametrization of subgrid scale vertical momentum transport had a more direct effect. With the mass flux scheme a parametrization for vertical momentum exchanges by cumulus convection was introduced. In the tropics, where its major impact is felt, the so called parametrized cumulus friction produces a down gradient momentum flux which, in general, decelerates the flow in the upper troposphere.

Momentum budget studies and forecast experiments had shown that the first version of the ECMWF gravity wave drag scheme produced an excessive upper level drag and did not include boundary layer dissipation processes which were found in observational studies and in very high resolution mesoscale models. These defects were taken into consideration in the modified gravity wave drag scheme and the vertical distribution of the gravity wave stress was changed to reduce the upper level drag and introduce an additional low-level drag.

2. THE BUDGET RESIDUAL APPROACH

After more than a year of operational use we are in a position to examine the impact of these revisions on the momentum budget in different seasons. For this investigation of systematic forcing errors we make extensive use of short range forecast errors. Maps of systematic errors for the medium or extended range are generally less helpful since they show the integrated response to remote as well as local model errors. This is illustrated in Fig. 1 which shows the zonal mean 5 day forecast errors for the zonal wind and for the temperature in July 1989 and January 1990. In both seasons we see the common problem of an intensified and poleward shifted subtropical jet and upper level easterly errors in the tropics. A comparison with the temperature errors shows that an error in the meridional gradient of the temperature corresponds to an error in the vertical gradient of the wind. Thus the zonal mean errors satisfy, to a good approximation, the thermal wind equation which makes it difficult to separate the effect of thermal and mechanical forcing errors.

From the similarity of extended range errors to medium range errors we can assume that the shown monthly zonal mean errors at day 5 are to a large extent independent of initial errors and reflect problems in the thermal and mechanical forcing. Errors at day 1 (Fig. 2 a and b) are more closely related to local errors. However, they are still affected by adjustment processes which act only on a time scale of a few hours. Additionally we have to

take into account analysis and initialization errors. The similarity of many features in the day-1 and the day-5 errors suggests, however, that even after 24 hours we are seeing the response to forcing errors of the model.

The shortest integrations which can be verified against analyses are the 6 hour forecasts produced four times per day during the data assimilation where they serve as a first guess for the analysis. The zonal mean errors for this time range (Fig. 2c and 2d) look very much like the 24 hour forecast errors. However, the separation into errors of momentum and thermal forcing is still hampered by adjustment processes.

Taking the approach of diagnosing forcing errors from short range forecast errors to its extreme limit we have calculated the monthly mean initial tendency errors. As in Klinker and Sardeshmukh (1987) this is simply done by running the first, or without loss of generality the first few steps, of the operational model from all available analyses of a month (4 analyses per day). The initial tendency error is then obtained as the difference between the monthly mean initial model tendency and the observed tendency. This is equivalent to performing a budget study with exactly the same equations for momentum, temperature, and moisture and with the same analysis as being used in the operational model. Apart from small errors arising from the difference technique a budget residual calculated this way would be the same as the monthly mean model tendency errors. The diagnostic approach of calculating initial model tendencies is used here because it has an enormous advantage for isolating local model or data problems.

Though analysis or initialization errors play an even larger part for the initial tendency than for forecasts of 6 or 24 hours, it is surprising to find still a similar structure in the residual of the initial tendencies (Fig. 2e and 2f). In July and January a westerly budget residual in the upper troposphere at middle latitudes appears as a westerly error in the day-1 and the day-5 forecasts. A well known problem in the tropics, easterly wind errors at upper levels, is already evident from the initial tendency errors. From the similarity of the initial errors to medium range forecast errors we draw the conclusion that a substantial portion of the initial tendency errors is related to model forcing errors. Thus despite the presence of some analysis errors we are able to diagnose model forcing errors from budget residuals.

3. MOMENTUM ERRORS RELATED TO CUMULUS CONVECTION

The initial tendency errors in the zonal mean flow indicate a problem in the model's momentum forcing in the upper tropical troposphere. In order to gain a better physical understanding we investigated the geographical distribution of momentum errors and their possible link with the parametrization of vertical momentum fluxes. First we discuss the initial and 24 hour forecast errors of momentum and their dependence on thermal and mechanical forcing for January 1990. This will be followed by an assessment for different seasons.

3.1 The tropical momentum budget in winter

The largest tropical wind errors are found in all seasons in the upper tropical troposphere. The initial model tendencies and forecast errors are therefore shown for a layer in the upper troposphere. Fig. 3a shows the budget residual and Fig. 3b the parametrized terms of the momentum equation as a pressure weighted average over three model levels which represent a layer from 250 to 140 hPa. The momentum forcing at these levels in the tropics arises mainly from the parametrized vertical momentum flux in regions of deep convection. The direction of the forcing is roughly opposite to the vertical wind shear (Fig. 3c) between the upper and middle troposphere.

In general the horizontal structure of the monthly mean tendency error, the so called budget residual, is quite different from the structure of the momentum forcing itself. Only

where the direction of the forcing agrees with the direction of the residual can we assume that the parametrized forcing contributes to the budget residual. This is the case over northern parts of South America where the budget residual and the momentum forcing have an easterly component. Also the change in the orientation of the momentum forcing from an easterly direction in the northern parts of South America to a northwesterly to northerly direction in more central areas is reflected in a change of the direction of the budget residual with a larger northerly component. A second area of deep convection, where the direction of the budget residual corresponds to the direction of the momentum forcing, is in the Indonesian region. However, there the maximum momentum forcing is located more to the south than the maximum of the momentum residual.

The residual along the south-east coast of South America does not arise from a corresponding momentum forcing at all. As the parametrized forcing is very small in this area, an error in the initial conditions is the most likely cause. Over some areas of South Africa the budget residual has a sign which is opposite to the sign of the momentum forcing which would indicate that the budget residual in this area would be even larger without cumulus friction.

3.2 Initialization errors

The difference between the budget residual and the model's forcing shows that some errors in the initial tendencies must come from the adiabatic tendencies in the momentum equation. Assuming that the adiabatic part of the model formulation, the description of the advection, the coriolis term and the pressure gradient term, have only relatively small errors, errors obtained arise mainly from errors in the initial conditions. Possible sources are errors from the first guess which are only partly corrected by the analysis in an area of sparse data. A further and probably similar error compared with the first guess error arises from the fact that the same forcing which might have produced first guess errors is used in the initialization.

How an error in the diabatic forcing can affect the initial tendencies can be illustrated with the quasi-geostrophic diagnostic equation for the mean meridional circulation.

$$f_0^2 \psi_{pp} + R(-\Theta_p \psi_y)_y = f_0[u^* v^*]_{yp} - R[v^* \theta^*]_{yy} - f_0[M]_p + R[Q]_y \qquad (1)$$

The meridional streamfunction ψ is defined such that $[v]=\psi_p$ and $[w]=-\psi_y$. [M] and [Q] represent the zonally averaged diabatic momentum and heat forcing and Θ a standard value of the potential temperature θ. The use of the diabatic tendencies from the first 2 hours of the forecast in the ECMWF initialization scheme (Wergen, 1987) ensures a balance between the meridional streamfunction and the zonal mean diabatic forcing similar to, but even better than the balance in equation (1) for quasi-geostrophic scaling. Thus without going into the details of diabatic normal mode initialization we can explain that an error in the diabatic heating [Q] or in the momentum forcing [M] would imply an error in the meridional streamfunction ψ. Klinker and Sardeshmukh (1987) have shown that the use of an excessive momentum exchange by vertical diffusion in the free atmosphere leads to an erroneous adjustment of the meridional circulation during the initialization which compensates a part of the budget residual via the f[v] term. Thus the diagnosed budget residual from the initial model tendencies showed only a part of the real momentum forcing problem.

For the interpretation of momentum errors in the tropics we investigated the impact of thermal forcing errors during the initialization. In order to estimate the local effects on the initial tendencies we have carried out an initialization experiment. From the diagnosis of the

heat budget we found that the model has a tendency towards excessive diabatic heating over land. The vertical integral of the budget residual for the sensible heat for January 1990 (Fig. 4) suggests that the condensational heating rates in the cumulus convection are too large. A comparison against observed rainfall confirms that the model produces excessive rainfall rates in the first 24 hours of the forecast.

In the initialization experiment we have reinitialized the monthly mean mass and wind field of January 1990. This was done by running the model from the monthly mean upper air and surface fields to provide the initial adiabatic tendencies and the diabatic tendencies of the first two hours which are both required in the diabatic normal mode initialization. To the model's diabatic tendency we have added the diagnosed monthly mean temperature budget residual as an error forcing term. The initialization provided an adjustment of the wind and mass field to balance the large scale flow with the total diabatic forcing including the additional thermal error forcing. From this initialized state one forecast step has been carried out in which the error forcing was excluded. In a control experiment the error forcing was excluded from the initialization and the first model step.

Thus the two initial tendencies after the initialization differ only because the initial states are slightly different as a consequence of a thermal error forcing used in one initialization but not in the other. We term this an initialization error. Fig. 5 shows the contribution of this error to the upper troposphere (140 to 250 hPa), which should be compared with the ensemble initial tendency error of the month (Fig. 3a). Note that the tendency vectors are drawn on the basis of a unit length which is only 50% of the unit length used for the budget residual.

The similarity between the momentum budget residual and the influence of a thermal forcing error on the initialization is striking. Over two major convection zones, northern South America and South Africa, the initialization error has the same direction as the budget residual. Along the south-east coast of South America the initialization error explains why we found a budget residual in the momentum budget in that region where no model momentum forcing takes place. The comparison suggests that a large part of the budget residual is indeed the result of errors in the thermal forcing.

3.3 Short range forecast errors

The effect of diabatic forcing errors on the wind field during the initialization and their subsequent influence on the initial momentum tendencies is similar to their effect on short range forecast errors. We have simulated the forecast impact by inserting the heat budget residual as additional constant forcing in a one day integration. As with the initialization experiment we used a monthly mean as initial state for this forecast and carried out a control forecast from the same initial conditions with no additional forcing.

Fig. 6a shows the impact of the thermal error forcing on the upper tropospheric flow. Over northern parts of South America the thermal forcing produces an easterly flow with an anticyclonic circulation further to the south and to the north. This error pattern corresponds very much to a steady-state solution of the shallow-water equations for an isolated heat source close to the equator (Gill, 1980). Further characteristics of the steady state solution, upper level westerlies due to Kelvin waves east of the heating and upper level easterlies due to Rossby waves west of the heating, can also be found in connection with the heating error over northern parts of South America.

Comparing the 24 hour response of the upper tropospheric flow (Fig. 6a) with the 24 hour operational forecast error for the month (Fig. 6b) we see a large similarity in the tropics. Especially over South America and South Africa the heat forcing reproduces very closely the ensemble day-1 forecast error. Larger differences are seen over Indonesia. Here the budget

residual for sensible heat is much smaller than over land, which means that momentum forcing errors have a more direct influence on short range momentum errors.

3.4 Seasonal variations

From the results of the initialization experiment and from the short range forecast experiments we can conclude that errors in the thermal forcing contribute significantly to tropical easterly errors. The role of the parametrized momentum exchange in the mass flux scheme for momentum errors depends very much on the season. During the summer the momentum forcing by cumulus convection (Fig. 7b) is much stronger than during the winter as shown in Fig. 3b. Due to the upper level easterly jet over Africa, India and South-East Asia the vertical shear in these areas is easterly (Fig. 7c). Thus the momentum exchange in the convectively active areas causes a deceleration of the upper level easterlies. Judged from the orientation of the initial tendency errors (Fig. 7a) and the parametrized forcing, cumulus friction would explain a part of the budget residual over India and South-East Asia. Over Central Africa the budget residual would be larger without cumulus friction. In central parts of South-America the vertical wind structure is quite different. An easterly momentum forcing in the presence of a westerly shear contributes to a easterly budget residual there.

In April (Fig. 8a to c) the position of areas of convective activity relative to the subtropical jet is different from the other two months considered here. The major convection occurs now in regions with a rather large westerly wind shear which leads to a predominantly easterly acceleration of the upper level flow by the momentum exchange of the mass flux scheme. The forcing is particularly large in latitude bands around 20°N and 5 to 20°S. These are the same regions where errors from the thermal forcing create a relative large Rossby wave response with upper level easterly wind errors.

Thus the benefit of the momentum part of the mass flux scheme depends very much on the season. The largest positive impact on the zonal mean easterly errors was found in earlier experimentation in the summer which corresponds to the fact that during the presence of the tropical easterly jet at upper levels the momentum exchange of the mass flux scheme produces quite a strong westerly forcing. This westerly forcing tends to dampen easterly errors which are generated by the Rossby wave response of thermal forcing errors. In a situation where a strong westerly vertical wind shear is present in convectively active areas, errors from the heat forcing are enhanced by the parametrized momentum exchange of the mass flux scheme.

3.5 Conclusions

The diagnosis of initial model tendencies and short range forecasts has pointed to the major sources of tropical momentum errors. This has been achieved despite the fact that the interpretation of momentum budget residuals in the tropics is hampered by the presence of relatively large diabatic heating errors. As the initialization creates a balance between the total diabatic forcing and the wind field, errors in the diabatic heating rates of convection cause errors in the initial momentum tendencies. By using the budget residual of sensible heat as a form of error forcing in the initialization it could be shown that large parts of the initial momentum tendency errors are indeed caused by thermal forcing errors. In a similar way the use of the temperature residual in a 24 hour forecast run from a monthly mean state suggests that a large part of short range momentum forecast errors are the result of thermal forcing errors.

Apart from these secondary momentum errors there is evidence for a direct contribution of the parametrized momentum transport of cumulus convection to the momentum residual. The negative impact of cumulus friction is particularly large when the vertical shear is westerly.

The general tendency of thermal forcing errors to produce upper level easterly wind errors is then enhanced by the cumulus friction. However, in the presence of an upper level easterly jet like in the summer over a wide area from West Africa to South East Asia cumulus friction tends to oppose the general tendency of the model to produce a zonal mean easterly error.

The largest momentum residuals are found at the outflow level of deep convection. This points to the uncertainty in defining a realistic 'in-cloud' momentum profile. It is hoped that an improved profile can be gained by accounting, in a dynamically consistent manner, for the cloud induced pressure field.

4. MOMENTUM ERRORS RELATED TO SUBGRID SCALE OROGRAPHIC FORCING

The first investigation in which the budget residual technique was used to diagnose systematic errors in the model's momentum forcing (Klinker and Sardeshmukh, 1987) revealed large imbalances in the initial momentum tendencies of the stratosphere over the Rocky Mountains and the Himalayas. These errors could be related to an excessive momentum forcing from the parametrization of gravity wave drag. Additional model integrations showed that a reduction of the upper level gravity wave drag had a beneficial impact on the predicted flow in the stratosphere. From recent experiments with high resolution mesoscale models and from observational studies there is some evidence that gravity waves exert a larger low level drag on the atmosphere than was assumed in the first parametrization of gravity wave drag used at ECMWF. These results have been taken into account for the modifications of the gravity wave drag scheme in May 1989. In view of the model change we have reexamined the initial model tendencies and short range forecast errors for January 1990. The relative role of envelope orography and gravity wave drag was also investigated by carrying out data assimilation experiments with different combinations of orographic forcing.

4.1 The vertically integrated budget residual for winter

Budget residuals have been calculated for four consecutive Januaries including January 1987 to January 1990. An average of the zonal mean budget residual for the first three Januaries indicates the excessive drag in the topmost three model levels (Fig. 9). The negative residual is located around 45 degrees north in the stratosphere where the maximum gravity wave drag is applied. Comparing the budget residual of the zonal mean flow before and after the parametrization change (Fig. 9 and Fig. 2e) we see a clear reduction of the upper level budget residual with the new scheme in January 1990 though a small residual is still left in the topmost level which develops into a upper level easterly error in the zonal mean wind within the first 24 hours of the operational forecasts (Fig. 2a).

The vertically integrated momentum equation can be used to diagnose errors in the surface stress. The contribution of the horizontal diffusion, which is not expressed as a vertical derivative, is relatively small for the scales considered here. The surface stress will include contributions from the turbulent stress in the boundary layer and from the gravity wave stress. The parametrized momentum flux for cumulus convection integrates to zero when integrated over the atmosphere. Therefore cumulus friction does not contribute directly to errors of the surface stress.

It was found that budget residuals based on initial model tendencies for a month may still have some nonsystematic component in the model's errors, this is particularly evident in maps of momentum budget residuals. Therefore, we have extended the budget residual calculations to the full winter season - December 1989 to February 1990. Fig. 10a shows the budget residual for the three Januaries 1987 to 1989, Fig 10b for January 1990 and Fig. 10c for the complete winter season 1989/1990.

For the last January the initial tendency errors are clearly reduced compared to the previous three Januaries. However, there is still a residual with maximum values over the major mountain ranges such as the Rocky mountains and the Himalayas. The largest values of up to 0.2 N/m^2 are reached over the Himalayas. The extension of the initial tendency calculations to the full winter season of 1989/1990 produces only a slightly modified result. Over the North Pacific and North Atlantic the westerly budget residual is more pronounced and over the Himalayas the easterly budget residual is reduced.

Stress errors diagnosed by integrating initial tendencies over the full atmosphere, of course contain errors from the boundary layer which are related to errors of the turbulent surface stress. In general the contribution of the boundary layer to the vertical integrated budget residual is relatively small as is shown in Fig 10d. Over land areas with flat terrain or low mountains the easterly budget residual in the boundary layer points to an overestimation of the turbulent stress. The small residual over high mountains suggests that the main part of the imbalance in the complete vertical integral arises from the free atmosphere above model level 15 which is roughly 850 hPa.

4.3 The effect of envelope orography on initial tendencies

One uncertainty in the interpretation of momentum budget residuals over mountains arises from the fact that the increase of the mountain height by a value proportional to the subgrid variance of the orography is a part of the parametrization of subgrid scale orographic effects. Therefore the question arises whether the residual over mountains is partly caused by the envelope orography.

An inexpensive solution to this problem would be to calculate the initial model tendencies with a changed mountain height or a changed gravity wave drag scheme. A large change in the physical forcing would, however, affect the initial balance of the model. Budget residuals should always be calculated from well balanced initial conditions. The best balance we can get with the present forecasting system at ECMWF is to use the same model formulation - including the appropriate boundary conditions over orography - in the data assimilation and for the initial model steps. Repeating a full data assimilation with a modified model formulation for a month is an expensive procedure.

For reasons of economy we have therefore restricted our investigation to a short period with a certain flow type from which we could expect a large impact from mountain forcing. A period of three days in January 1988 was chosen when a strong westerly flow crossed the Rocky Mountains close to the border between Canada and the USA (Fig. 11). The three data assimilation experiments were specified as follows: with envelope orography plus gravity wave drag (ENV); with mean orography plus gravity wave drag (MEAN); and with envelope orography excluding gravity wave drag (NOGWD). The summer 1989 model and analysis formulation were used in the data assimilation which thus included the gravity wave drag parametrization implemented in 1989.

In order to illustrate the effect of envelope orography on initial tendencies we have calculated adiabatic tendencies from both initial data sets, one created with the ENV-assimilation and one with the MEAN-assimilation. The adiabatic tendencies were then averaged over three days (four tendencies per day) and integrated in the vertical over the full atmosphere. Thus we can interpret the difference between the initial tendencies from envelope orography and from mean orography (Fig. 12) as changes in the surface stress caused by the envelope orography. In the presence of the rather strong cross mountain flow the impact of the increased mountain heights on the initial momentum tendencies corresponds to a surface drag which is almost perpendicular to the flow over the mountain crest. The influence of higher mountains is also in agreement with flow changes one would expect from the conservation law of potential vorticity.

This results is significant for the interpretation of the vertically integrated budget residual. As the direction of the budget residual is mainly parallel to the flow, it is unlikely that the increase of mountain heights would explain a large part of the obtained residual.

4.4 The effect of envelope orography and gravity wave drag on 6 hour forecast errors

The excessive upper level gravity wave drag in the first ECMWF version had a noticeable influence on the short range forecast errors in the stratosphere. Within a few hours the upper level flow adjusted to the mainly easterly drag with a deflection to the north. This was also seen in a comparison of 6 hour forecast winds against upper level wind observations.

For a verification of 6 hour forecasts with different model formulations of orographic forcing the advantage of performing full data assimilation experiments is obvious. For each type of subgrid scale mountain forcing in the assimilation (ENV, MEAN, NOGWD) we can verify the six hour forecast against its own analysis. Here we relate the vertically integrated 6 hour tendencies to surface stress problems.

Fig. 13 a to c shows the vertically integrated first guess errors for the ENV-, MEAN- and NOGWD-assimilation. In all assimilations we see in the 6 hour errors an anticyclonic error pattern south of the region where the westerly flow crosses the Rocky Mountains and a secondary cyclonic error pattern to the north. This error pattern suggests that in the analysis the cross mountain flow is weaker and the deflection of the flow around the mountain is stronger than in the 6 hour forecast.

4.4.1 Influence of orographic height

With the use of mean orography and gravity wave drag in the model, the 6 hour forecast errors clearly indicate the excessive cross mountain flow (Fig. 13b). In particular, the 6 hour forecast underestimates the deflection of the flow to the south on the windward side of the mountains and to the north on the lee side.

With the envelope orography and gravity wave drag in the assimilation the 6 hour forecast errors are reduced in the centre of the cross-mountain jet and to the north of the jet; the major anticyclonic error pattern to the south of the jet is however intensified.

The difference map between the ENV first guess errors and MEAN first guess errors shows the impact of envelope orography on six hour forecasts more clearly (Fig. 14a). In addition we have calculated the difference in the magnitude of the first guess wind errors (Fig. 14b). Positive values indicate where the first guess errors with envelope orography are larger and negative values where the errors from mean orography are larger.

Compared with the impact of the envelope orography on initial tendencies, the impact on the six hour forecast is similar. There is, however, already some adjustment within 6 hours which can be discerned. Where the westerly jet crosses the mountains the adjustment is such that a larger component of deceleration is working against the flow. The consequence is that the flow over the mountains is reduced and the flow component around the mountains is increased to the north of the westerly jet. The changes in the magnitude of the six hour forecast errors indicate that envelope orography mainly improves the cyclonic error pattern to the north of the jet and the mountain cross flow. Further to the south we see a predominantly negative effect from the envelope orography.

4.4.2 Influence of gravity wave drag

The use of gravity wave drag has a noticeably smaller effect on the 6 hour forecast than the envelope orography. With gravity wave drag the 6 hour forecast errors are smaller on the lee side of the mountains and to the south of the major westerly flow (Fig. 13c). Reduced errors can also be seen over the mountains of North-West Canada and Alaska.

When assessing the impact of gravity wave drag on the flow it is worth noting that the maximum drag (Fig. 16a) is not found where the jet crosses the Rocky Mountains but rather further to the south over the Sierra Nevada and to the north over North-West Canada. In these areas the subgrid scale orographic variance is particularly large. Over the Sierra Nevada the gravity wave drag reaches values of up to 3 N m^{-2}. The horizontal distribution of the stress due to gravity waves is therefore very much different from the stress due to turbulence in the boundary layer (Fig. 16b), which shows a much closer relationship to the strength of the low level flow.

Comparing gravity wave drag itself with its impact on first guess errors (Fig. 16a and Fig. 15a) we notice a relatively large adjustment in some areas. Around the Sierra Nevada mountains the extremely large values of stress produce a cyclonic response in the 6 hour forecast errors. As with the effect of envelope orography this turns out to be detrimental to the quality of the first guess in a region around the maximum stress (Fig. 15b). Further to the west in the lee of the Rockies the gravity wave drag produces a positive impact on the first guess errors. The same is true for the mountainous region of Alaska and North-West Canada where the changes of first guess errors (Fig. 15a) and the direction of the gravity wave drag (Fig. 16a) coincide. Here only little adjustment of the six hour forecast to the forcing is seen. Compared to the impact of the envelope orography, gravity wave drag does only little to improve the excessive cross mountain flow in the central jet area.

4.4.3 Influence of envelope orography and gravity wave drag on the upper level flow

Though the two parametrizations of subgrid scale orographic forcing have some similarities in their contributions to modify the flow across and around the mountains, there are important differences in the detail. Apart from the failure of gravity wave drag to decelerate the strongest flow across the Rocky Mountains the large drag over the Sierra Nevada mountains causes a detrimental adjustment of the six hour forecast. This effect is apparent in the lower troposphere but particularly in the stratosphere.

Fig. 17a shows the impact of envelope orography and Fig. 18a the impact of gravity wave drag on the 6 hour forecast errors at the top level of the model. The tendency for an improvement or deterioration of first guess errors for the same level can be judged from the differences in the magnitudes of errors (Fig. 17b and 18b). In general the influence of envelope orography on the upper level flow is smaller than the effect of gravity wave drag. As shown by Tibaldi (1986) envelope orography is mainly felt in the lower troposphere and acts in some ways as a low level drag.

Over North America the gravity wave drag at upper levels creates an adjustment of the wind, similar to the adjustment at lower levels but on a larger scale. The deflection of the 6 hour forecast wind increases the first guess errors over a large area in the stratosphere. Over the Himalayas a small improvement can be seen from the envelope orography but a substantial improvement from the gravity wave drag scheme. The direction of the impact shows that the gravity wave drag scheme succeeds to oppose the tendency of the model to produce too strong stratospheric westerly winds over the Himalayas.

From the reduction of the upper level drag in the new gravity wave drag scheme we would expect a reduction of the adjustment of the stratospheric winds which we diagnosed especially over the Rocky Mountains. In Fig. 19 we compare the first guess errors of the operational scheme from January 1988 with the new scheme which has been used in the data assimilation experiment. Though some differences may also be due to differences between the old operational (January 1988 version) and the new analysis (summer 1989 version) which are not related to gravity wave drag, a clear signal emerges over the Rocky Mountains. The old scheme produced an adjustment of the stratospheric flow which was around 10 m s^{-1} larger than the new scheme, suggesting again that the upper level drag was too large in the old scheme.

4.5 Operational forecast errors

The first guess error structure found here over the Rocky Mountains for a three day period in January 1988 seems to be a typical error pattern for a certain flow type. We have investigated operational forecasts for the Winter 1989/1990 and found a relative large number of cases with a strong westerly flow over the Rockies. The average first guess error vertically integrated over the atmosphere for those cases (Fig. 20) shows a similar anticyclonic error structure as we found for the three day period in January 1988.

4.6 Conclusions

The data assimilation experiments showed some of the typical short range forecast errors occurring in a situation when mountain forcing is an important component in the momentum budget. It seems that the present parametrization of subgrid scale orographic process needs further improvements to simulate the modification of a flow passing over a mountainous terrain. In a flow type when the additional height due to subgrid scale orography is larger than U/N particles at low levels should be blocked by the mountains and the flow should be guided around the mountains themselves and around the 'wake' areas downstream of the mountains. Baines and Palmer (1990) have proposed a parametrization scheme in which the effect of flow blocking and wake creation would be achieved by a low level drag (C_D |U| U) applied between the surface and a level determined by the orography variance and the Froude Number of the flow. The replacement of the envelope orography by a low level drag would avoid the negative side effects which are caused by the increase of the total mountain volume over its actual value.

Comparing the first guess error pattern using mean orography (Fig. 13b) with the turbulent surface stress (Fig. 16b) indeed suggests that an increase of the low level drag proportional to the surface drag would probably have the desired effect of blocking the low level flow in the right place and creating a larger flow component around the mountains.

The momentum budget residual over mountains and the adjustment of the upper level flow to gravity wave drag suggest a reduction of the stress due to gravity waves. However this does not necessarily imply a further 'retuning' of the current gravity wave drag scheme itself. A low level drag parametrization which would be successful in creating a realistic deceleration of the flow over the mountains and in the 'wake' area would alter the input of the gravity wave drag scheme in such a way to reduce the total gravity wave drag.

References

Baines, P.G. and T. Palmer, 1990: Rationale for a new physically-based parametrization of subgridscale orographic effects. ECMWF Tech. Memo. No. 169.

Gill, A.E., 1980: Some simple solutions for heat-induced tropical circulation. Q.J.R.Meteorol.Soc., 106, 447-462.

Klinker, E. and P.D. Sardeshmukh, 1987: The diagnosis of systematic errors in numerical weather prediction models. Proceedings of a workshop on diabatic forcing held at ECMWF. 209-244.

Tibaldi, S., 1986: Envelope orography and maintenance of quasi-stationary waves in the ECMWF model. Adv. Geophys., 29, 339-374.

Wergen, W., 1987: Diabatic nonlinear normal mode initialization for a spectral model with a hybrid vertical coordinate. ECMWF Technical Report No. 59.

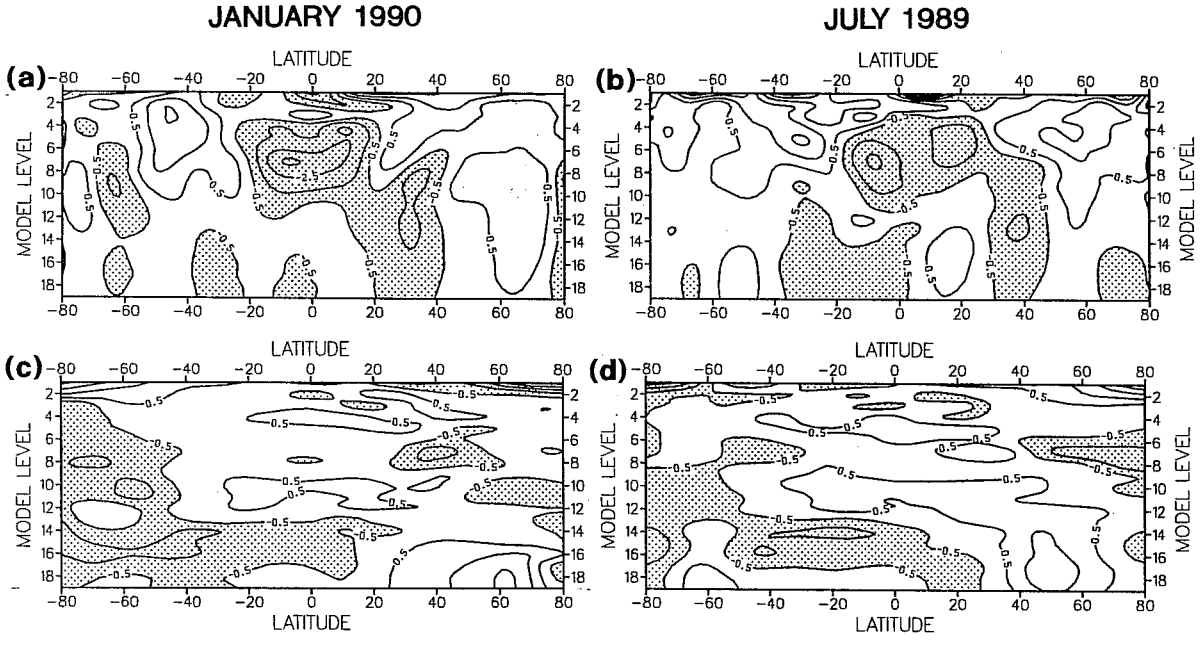

Fig. 1: Zonal mean day-5 errors for the zonal wind for January 1990 (a) and July 1989 (b). Units: ms^{-1}.
Zonal mean day-5 errors for temperature for January 1990 (c) and July 1989 (d). Units: K

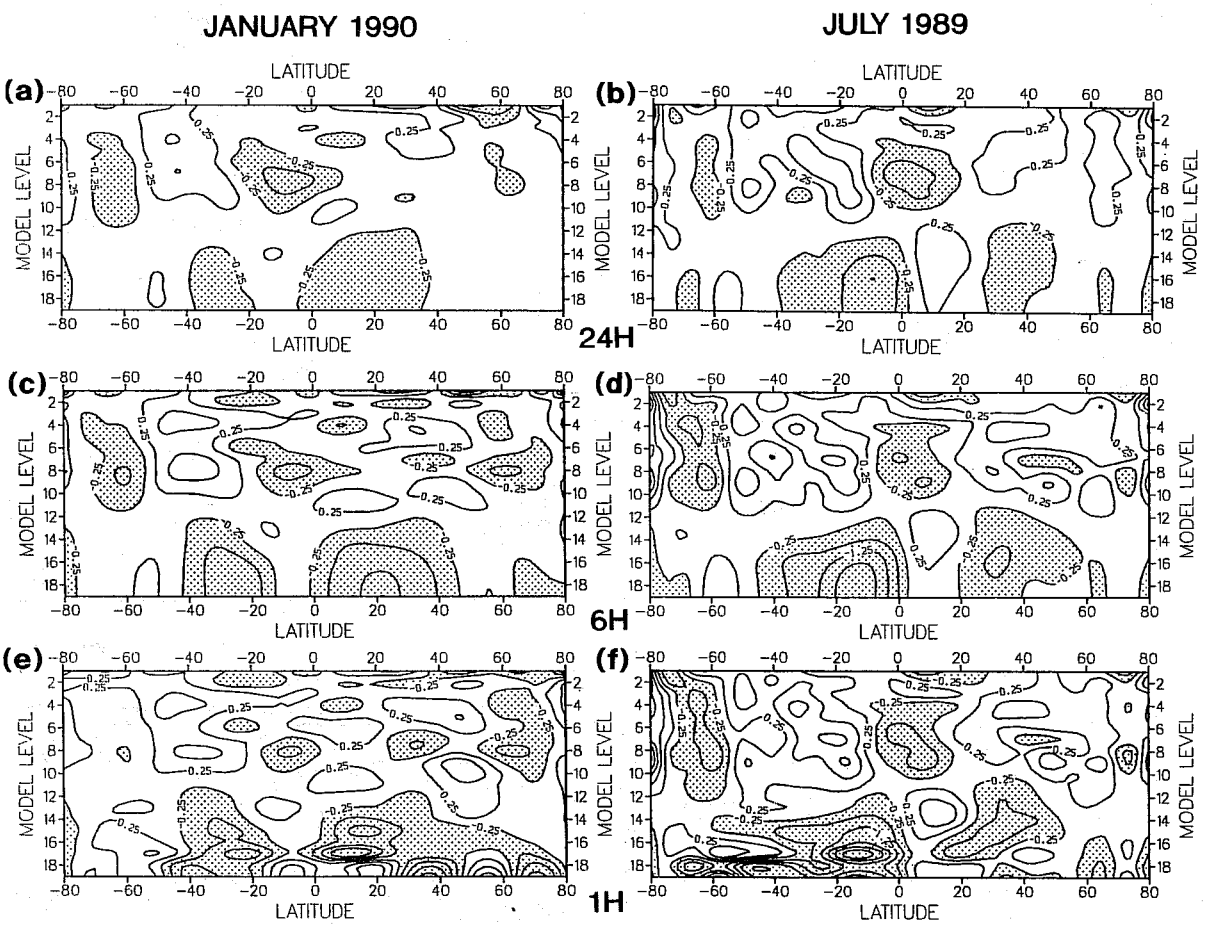

Fig. 2: Zonal mean errors of the zonal wind. Left column for January 1990, right column for July 1989. Top row: day-1 forecast errors. Middle row: 6-hour forecast errors. Bottom row: initial tendency errors. Units: $ms^{-1}d^{-1}$.

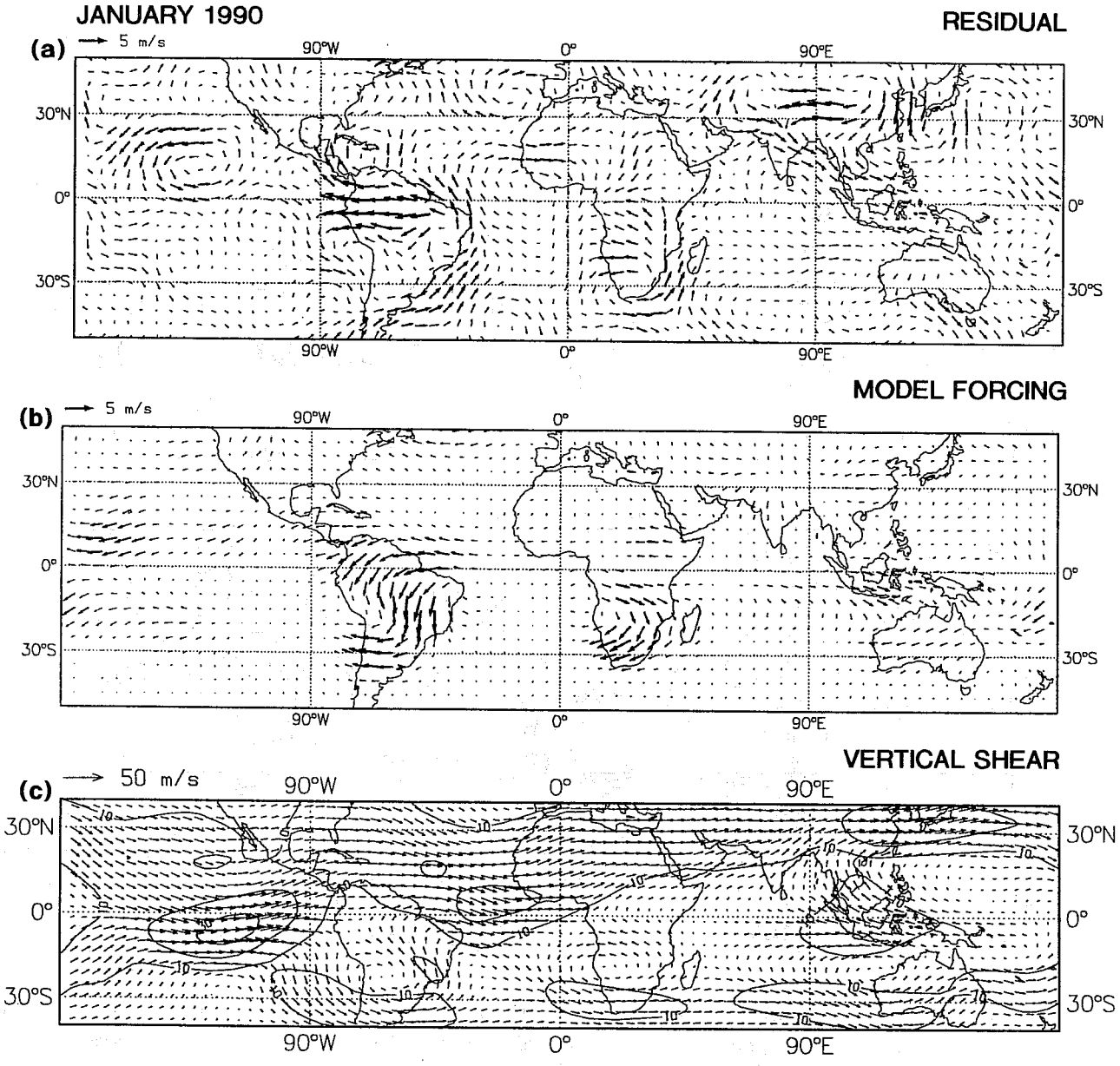

Fig. 3: Initial tendency errors (a) and momentum forcing (b) for January 1990. Pressure weighted average over model level 6 to 8 (140 to 250 hPa).
Units: $ms^{-1}d^{-1}$ (c) vertical wind shear between model level 6 and 11 (140 and 500 hPa)

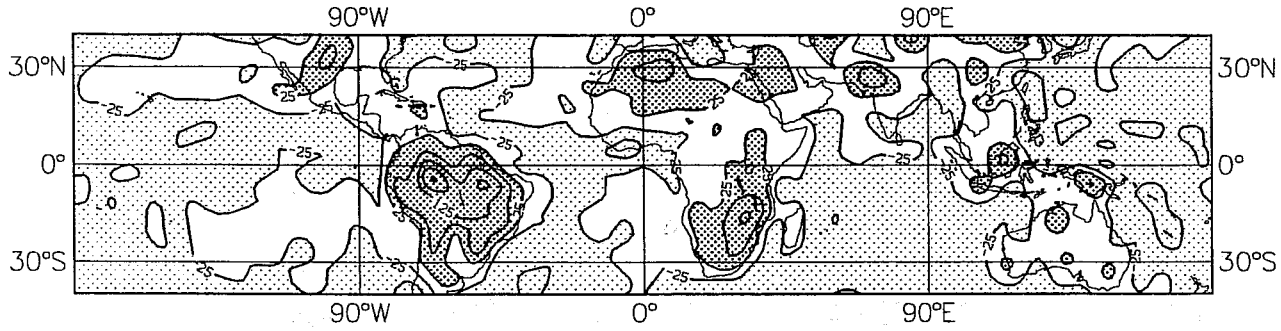

Fig. 4: Budget residual of sensible heat (cp*T) vertically integrated over the atmosphere for January 1990. Units: W m^{-2}.

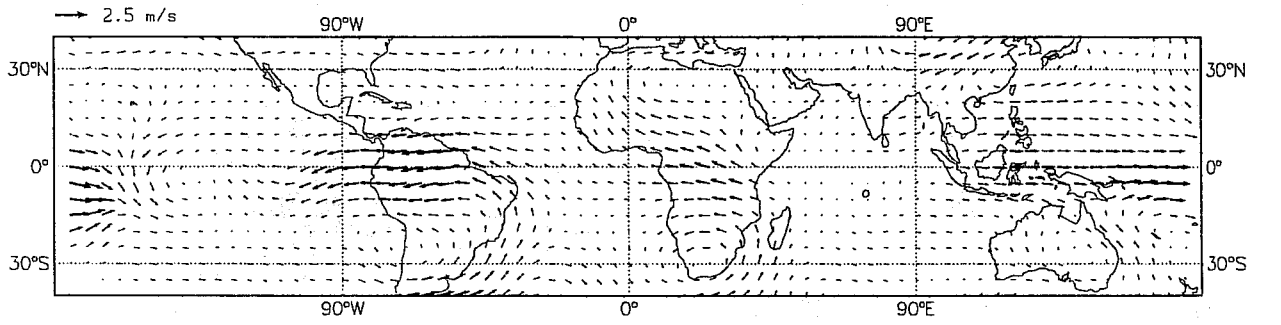

Fig. 5: Model tendency differences arising from initialization differences: tendency from initialized state using thermal forcing errors in the initialization only minus tendency from initialized state without using thermal forcing errors at all. Pressure weighted average over model level 6 to 8 (140 to 250 hPa).
Units: $ms^{-1}d^{-1}$.

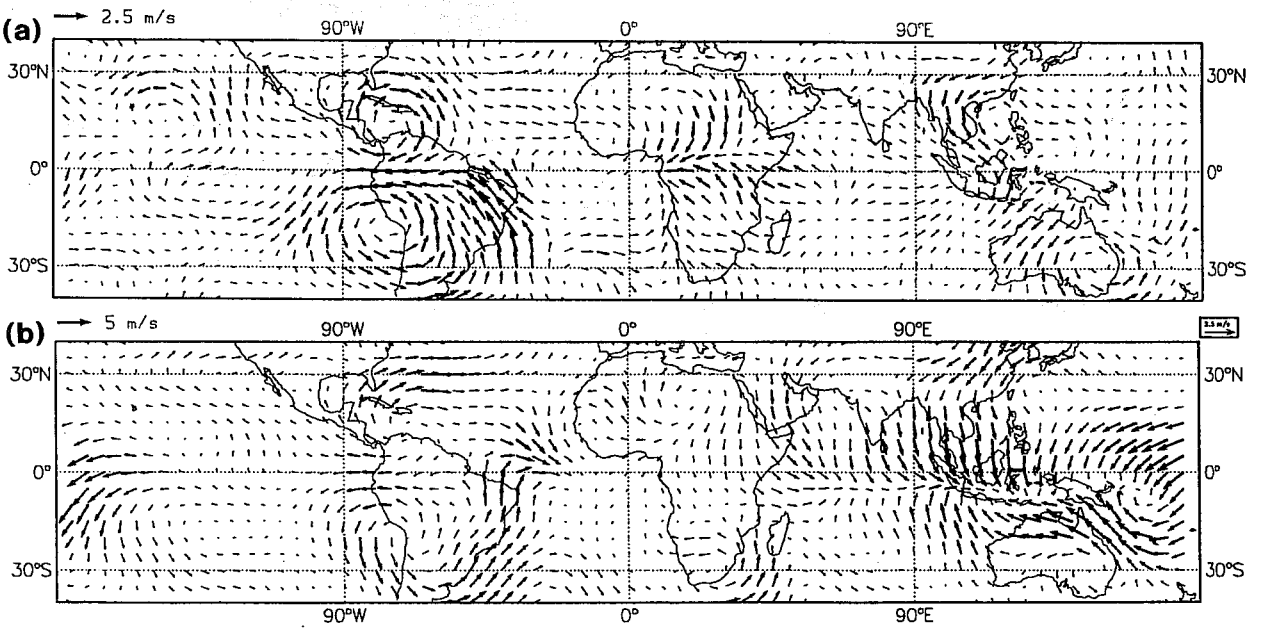

Fig. 6: (a) Difference between 24 hour forecast from monthly mean state with and without additional thermal error forcing. (b) Ensemble 24 hour forecast error for January 1990.
Pressure weighted average over model level 6 to 8 (140 to 250 hPa).
Units: ms^{-1}.

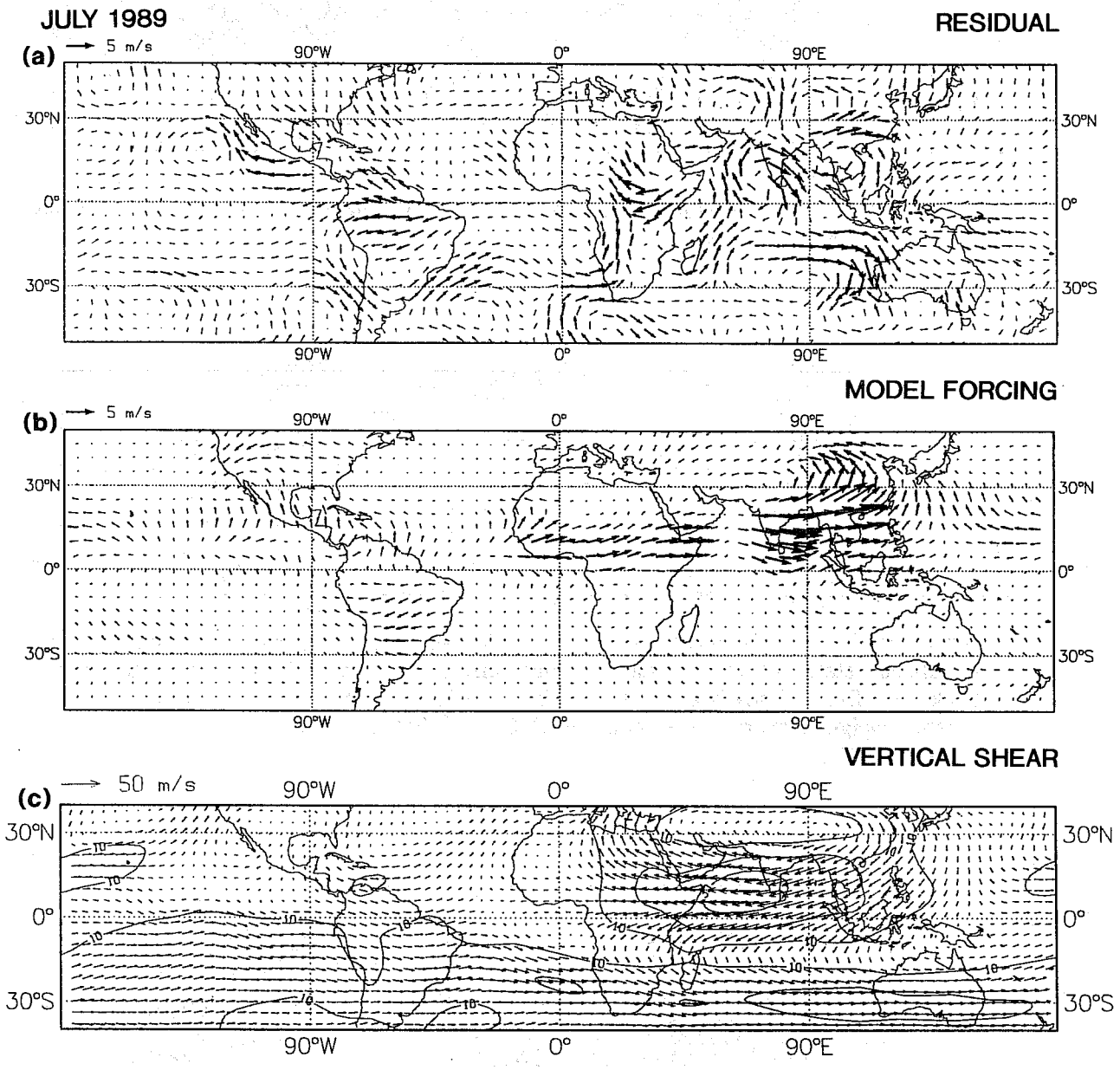

Fig. 7: Initial tendency errors (a) and momentum forcing (b) for July 1989. Pressure weighted average over model level 6 to 8 (140 to 250 hPa).
Units: $ms^{-1}d^{-1}$ (c) vertical wind shear between model level 6 and 11 (140 and 500 hPa)

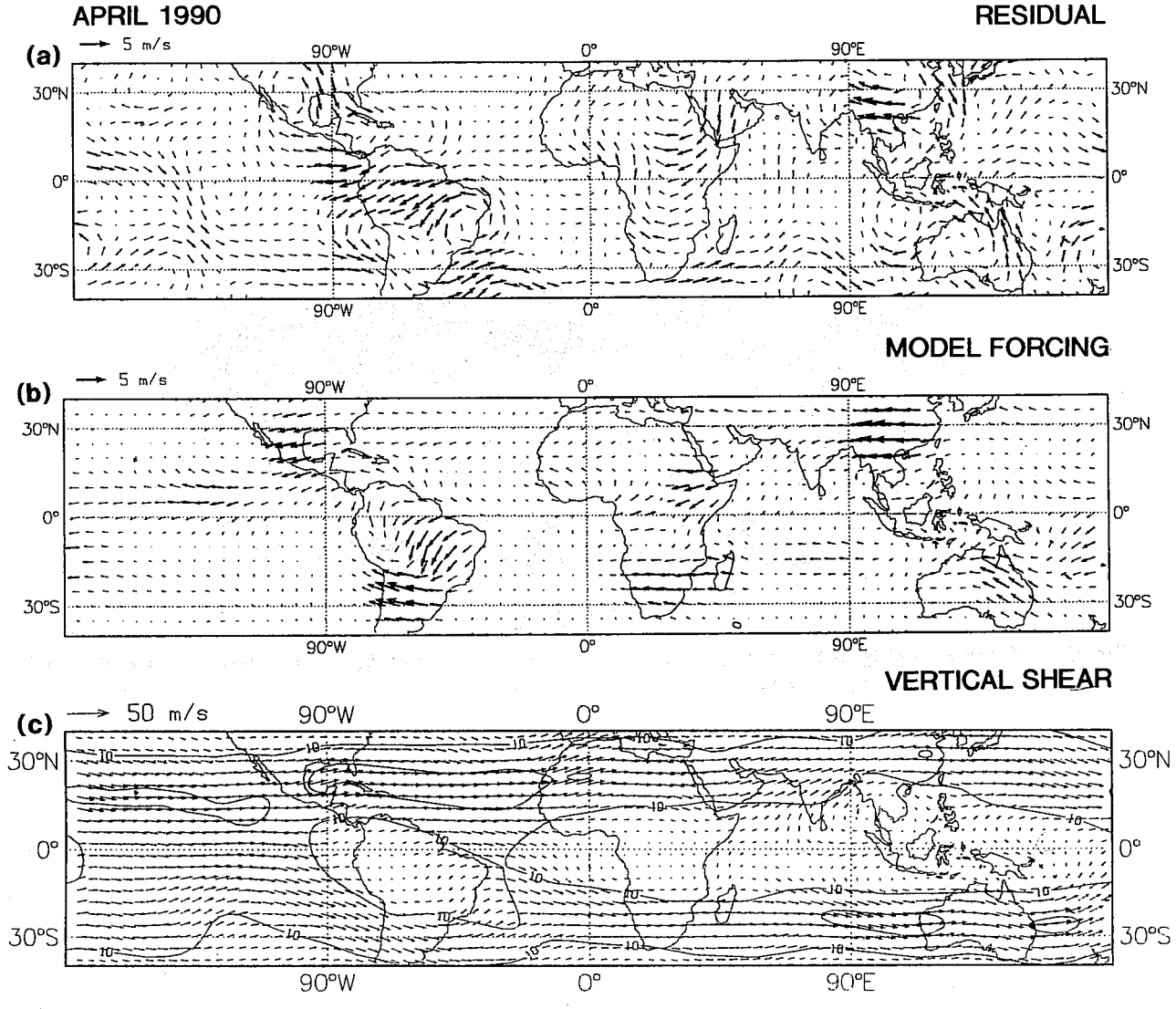

Fig. 8: Initial tendency errors (a) and momentum forcing (b) for a 10 day test period in April 1989. Pressure weighted average over model level 6 to 8 (140 to 250 hPa). Units: $ms^{-1}d^{-1}$. (c) vertical wind shear between model level 6 and 11 (140 and 500 hPa)

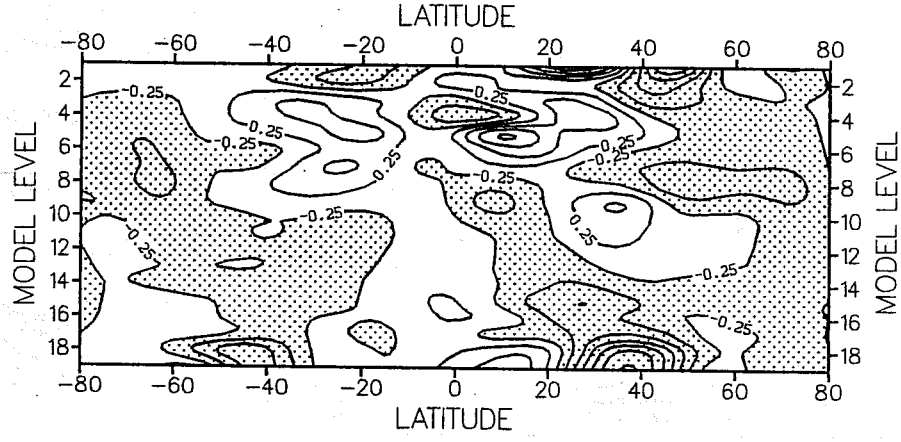

Fig. 9: Budget residual for the zonal mean wind as an average over January 1987, 1988, and 1989. Units: $ms^{-1}d^{-1}$.

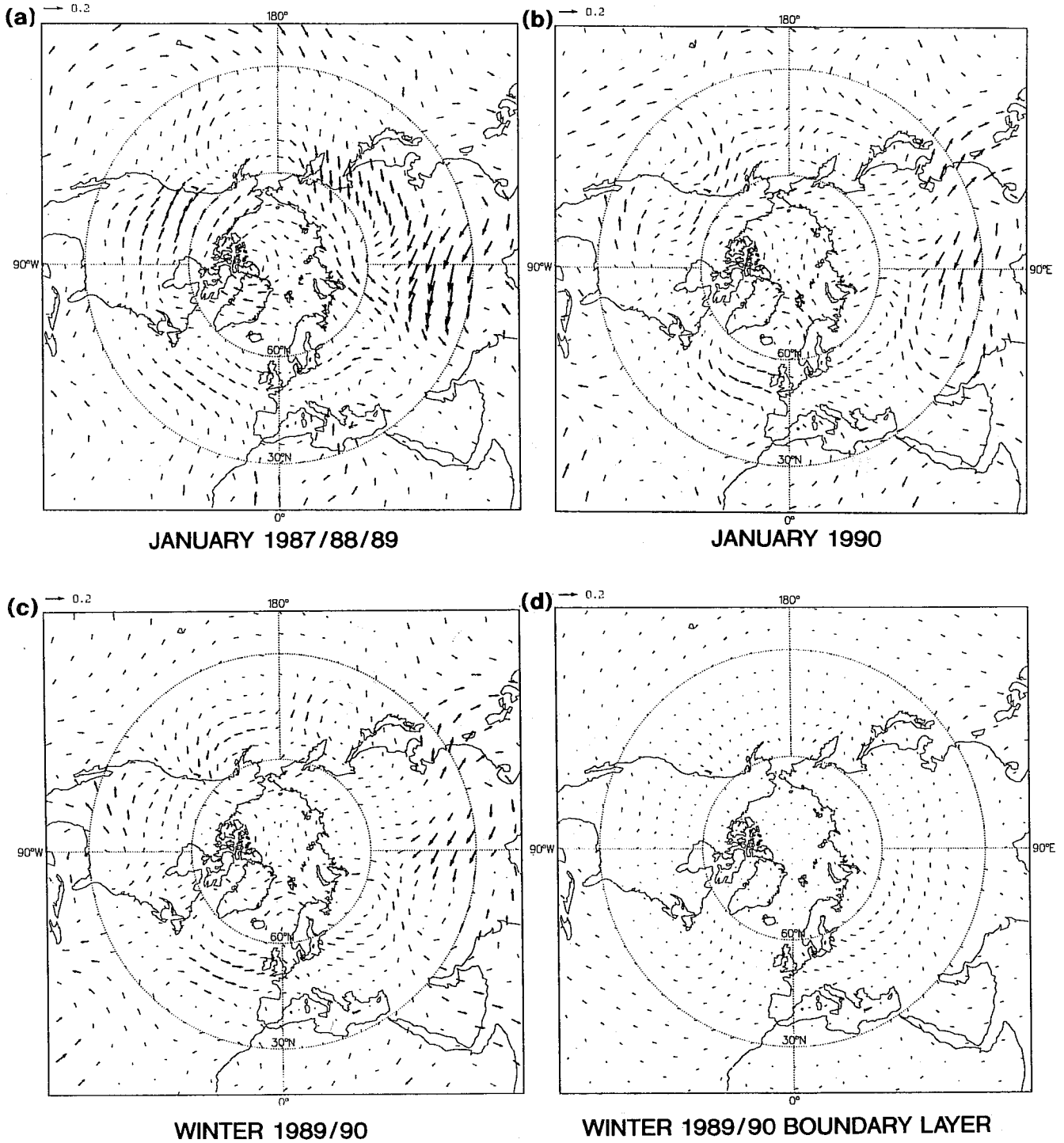

Fig. 10: Vertically integrated budget residual of momentum. (a) average over January 1987, 1988, and 1989, (b) January 1990, (c) Winter 1989/1990, (d) contribution of the boundary layer (model level 15 to 19) to the total integral for Winter 1989/1990. Units: $N\ m^{-2}$.

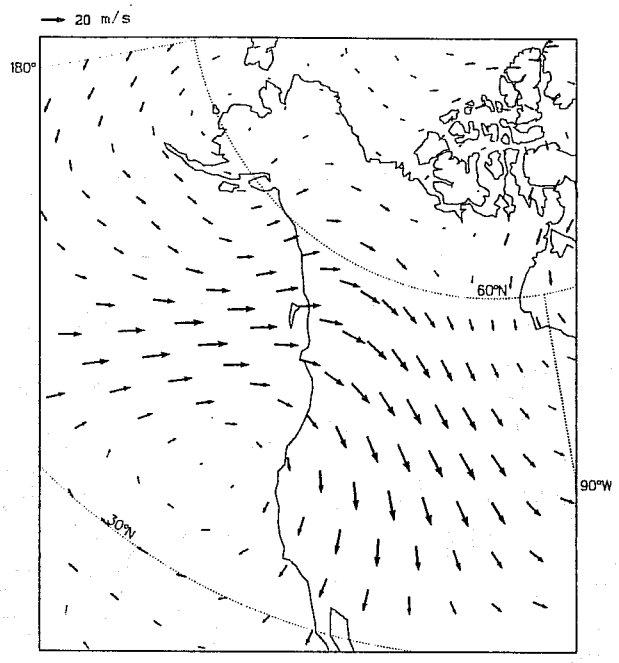

Fig. 11: Vertically averaged flow in the lower troposphere for a period of three days: 21.1.1988 to 24.1.1988. Units: ms^{-1}.

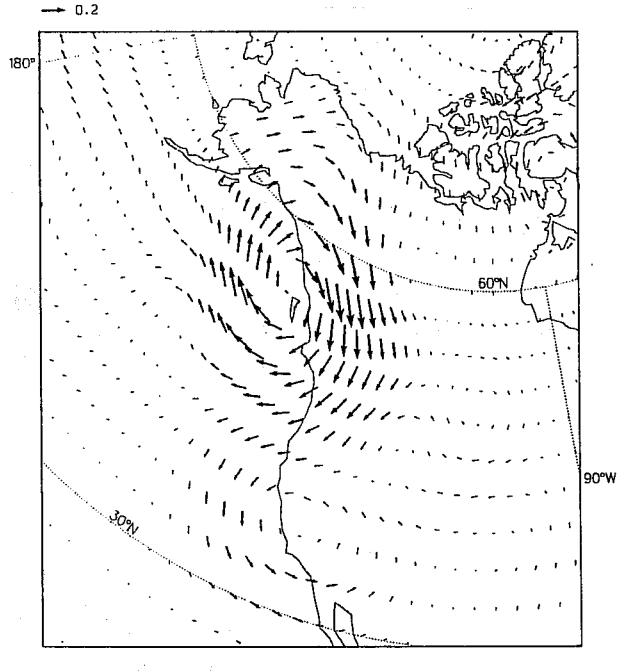

ENV-MEAN

Fig. 12: Initial adiabatic tendency difference integrated over the atmosphere. Difference between tendency from analysis with envelope orography and form analysis with mean orography. Average over three days. Units: $N\,m^{-2}$.

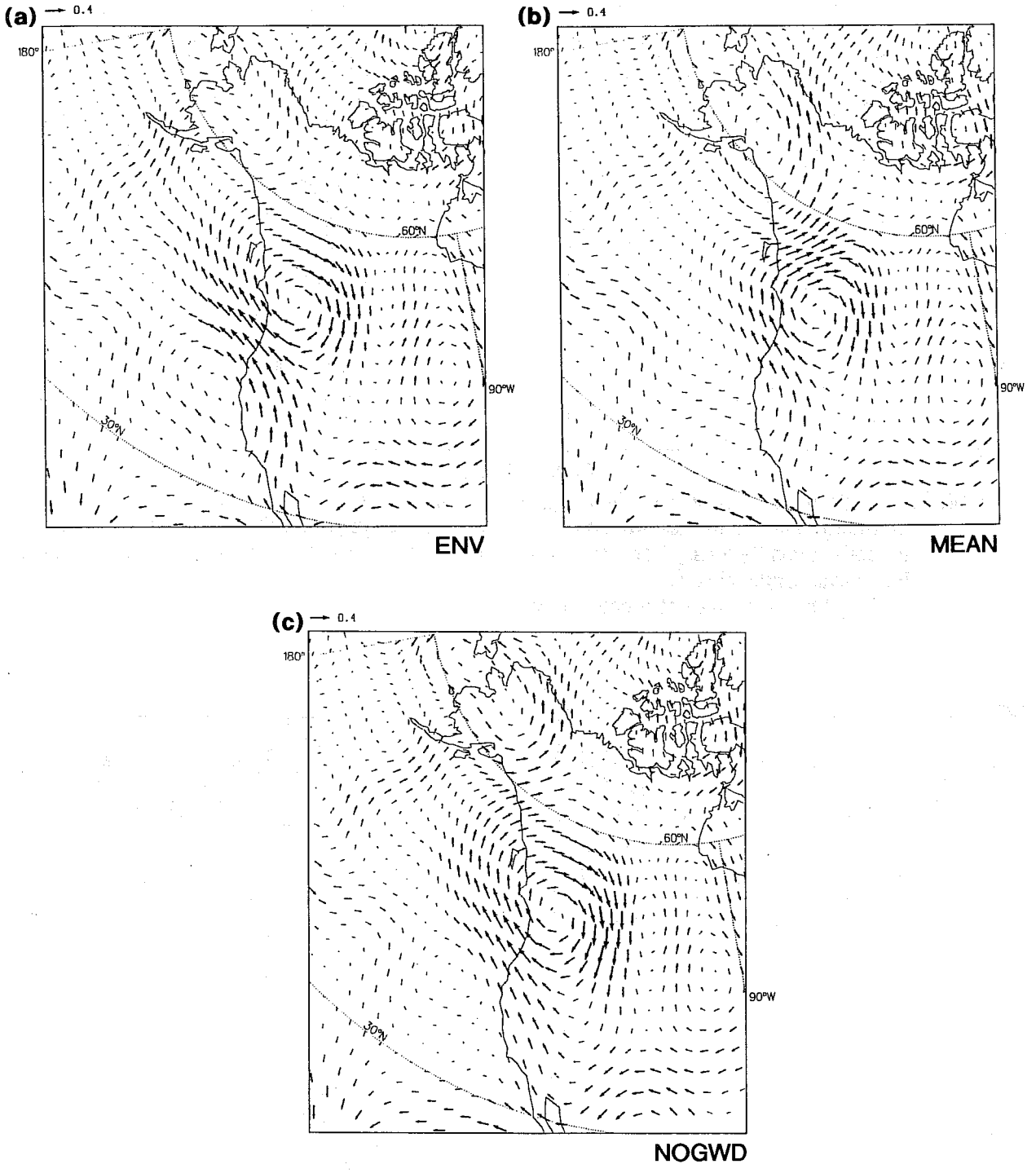

Fig. 13: First guess errors vertically integrated over the atmosphere and averaged over three days. (a) From assimilation with envelope orography and gravity wave drag. (b) From assimilation with mean orography and gravity wave drag. (c) From assimilation with envelope orography without gravity wave drag.
Units: N m^{-2}.

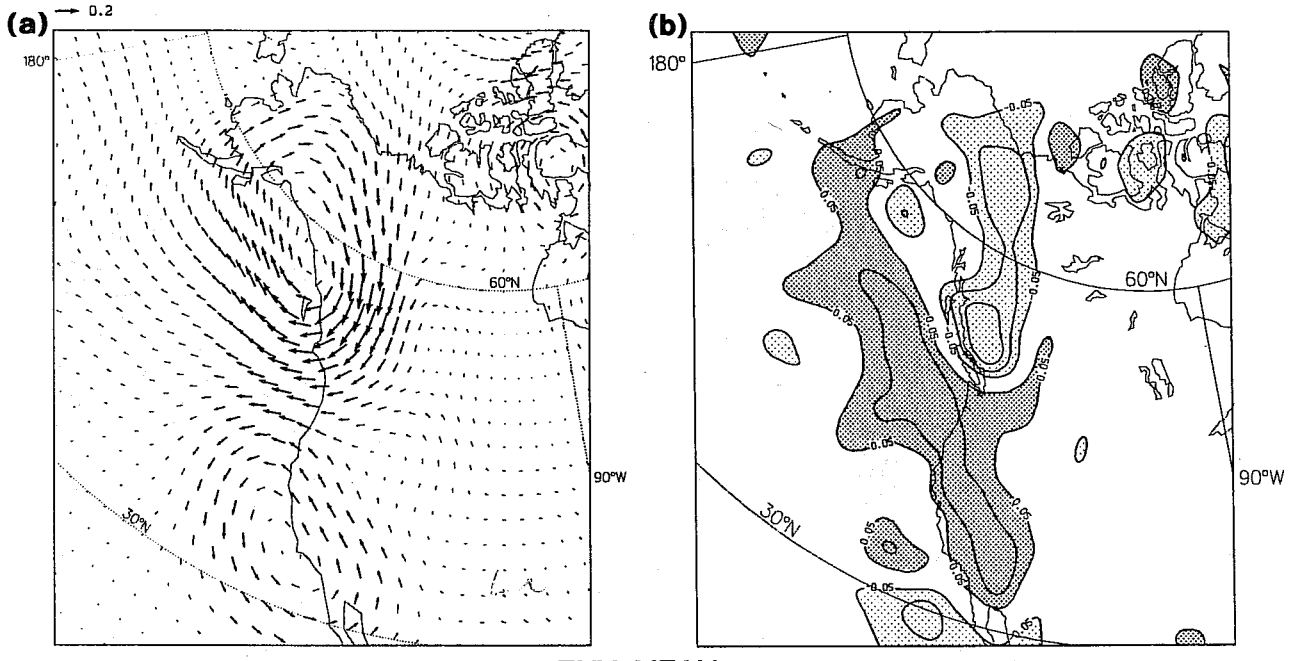

ENV–MEAN

Fig. 14: (a) Difference between first guess errors from assimilation with envelope orography and from assimilation with mean orography, gravity wave drag included in both assimilations. Vertical integral over the atmosphere and averaged over three days. Units: N m^{-2}.
(b) As (a) but difference of absolute errors.

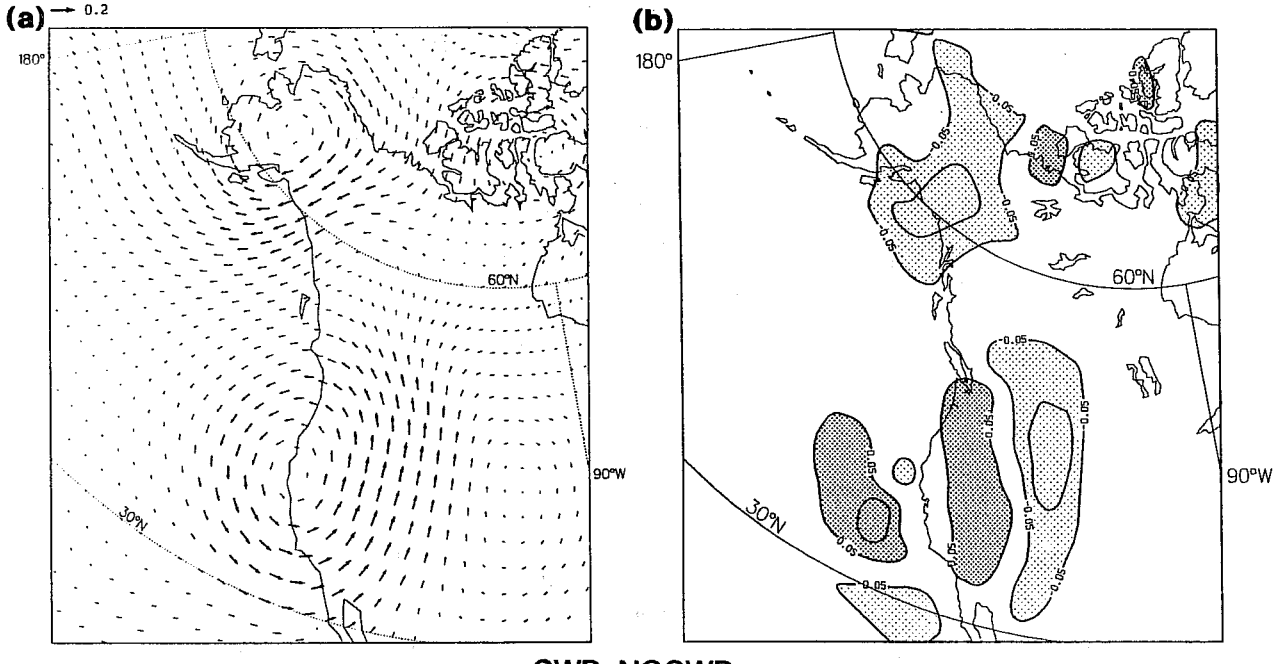

GWD–NOGWD

Fig. 15: (a) Difference between first guess errors from assimilation with gravity wave drag and from assimilation without gravity wave drag, both assimilations with envelope orography. Vertical integral over the atmosphere and averaged over three days. Units: N m^{-2}.
(b) As (a) but difference of absolute errors.

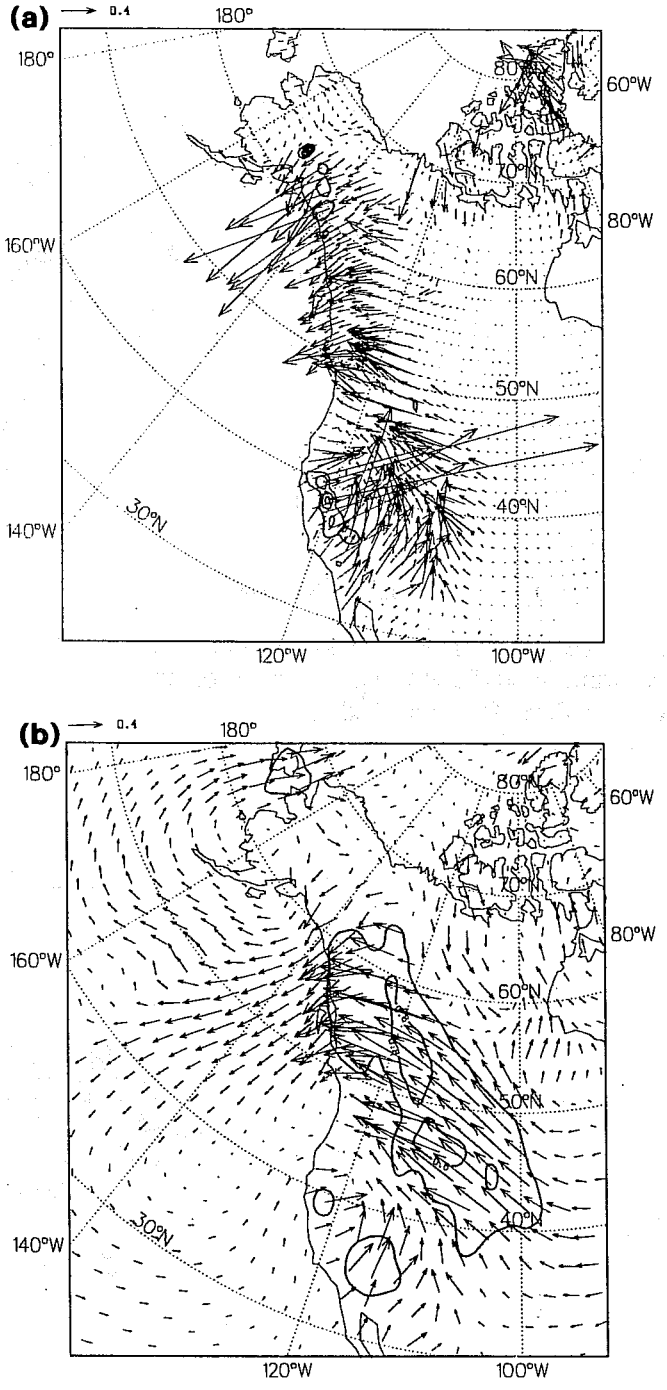

Fig. 16: (a) Gravity wave drag and (b) surface stress for the three day period (21. to 24.1.1988) Units: N m^{-2}.

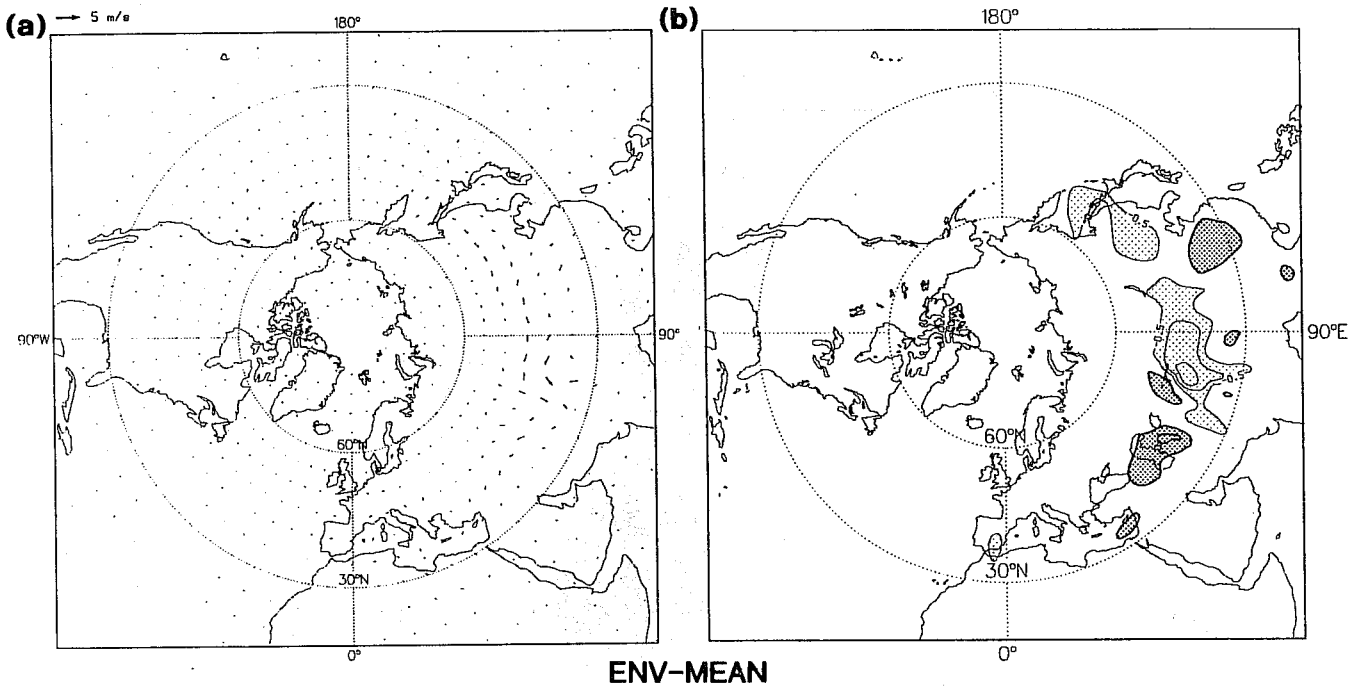

Fig. 17: (a) Difference between first guess errors from assimilation with envelope orography and from assimilation with mean orography for top model level (10 hPa). Averaged over three days. Units: m $s^{-1}d^{-1}$.
(b) As (a) but difference of absolute errors.

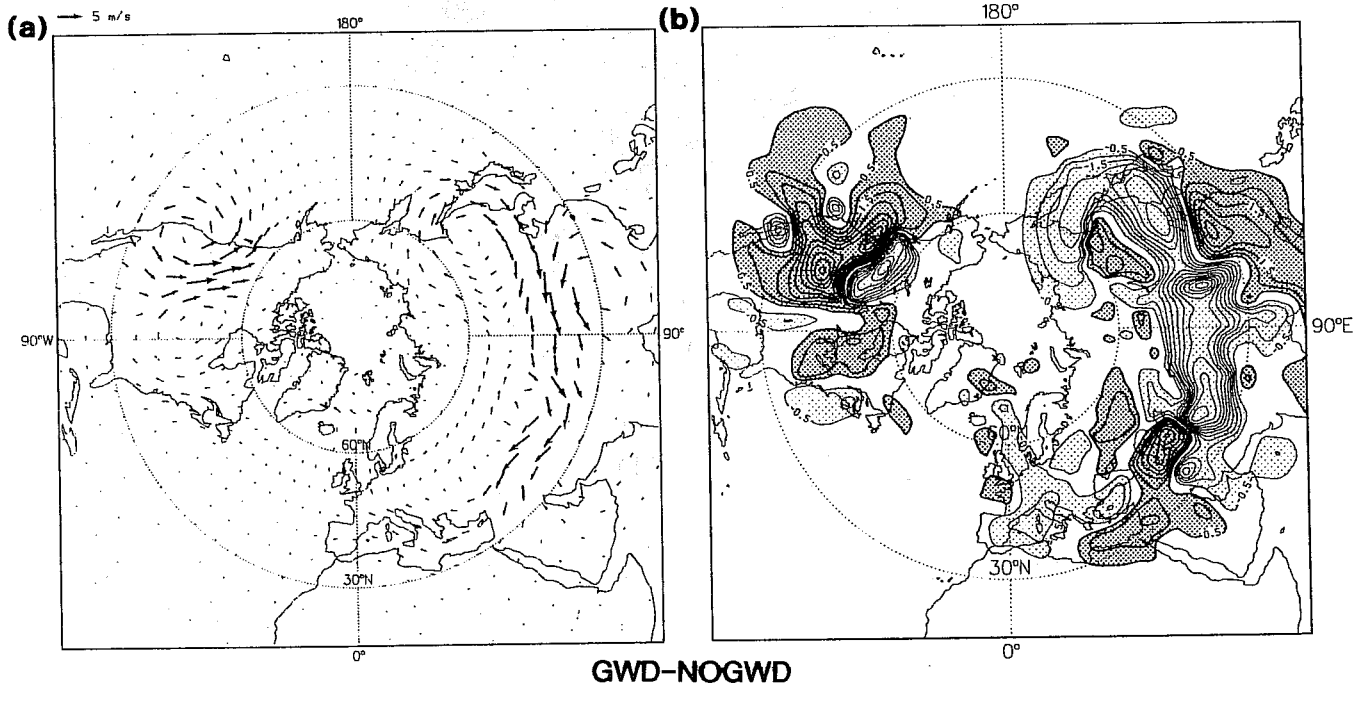

Fig. 18: (a) Difference between first guess errors from assimilation with gravity wave drag and from assimilation without gravity wave drag for top model level (10 hPa). Average over three days. Units: m s^{-1}.
(b) As (a) but difference of absolute errors.

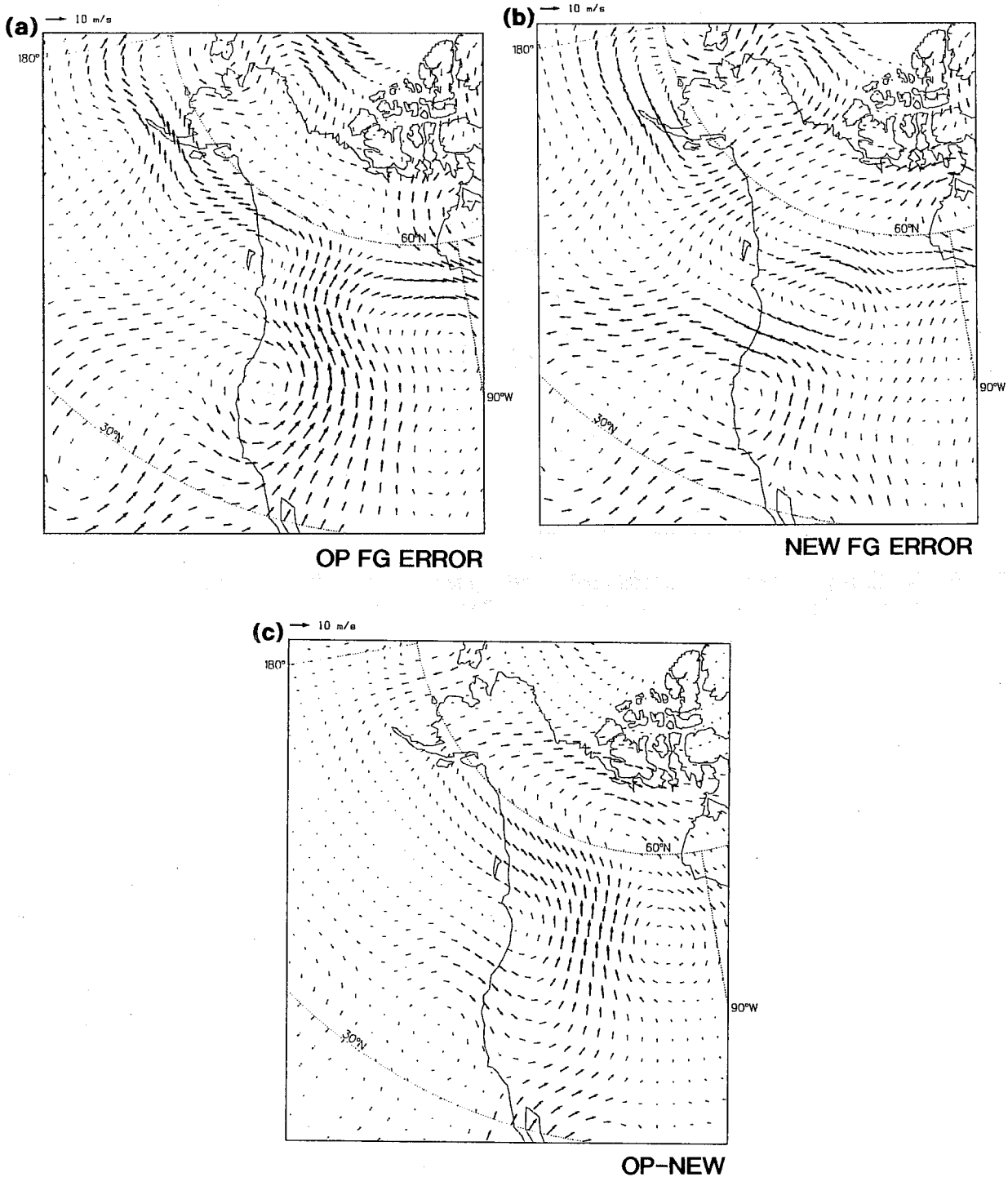

Fig. 19: First guess errors vertically averaged over the 5 top model levels (10 to 100hPa) and averaged over three days. (a) From the operational data assimilation (January 1988) with envelope orography and gravity wave drag. (b) From the new assimilation (summer 1989) with envelope orography and gravity wave drag. (c) Difference between (a) and (b). Units: m $s^{-1}d^{-1}$.

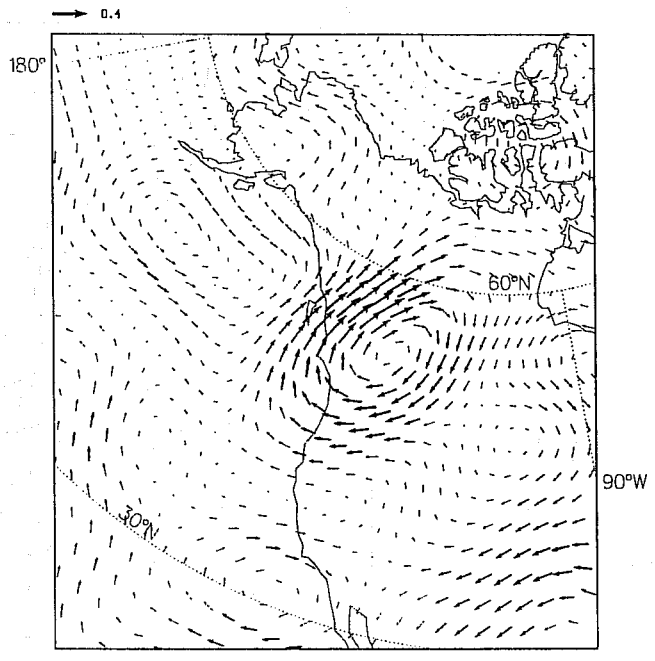

Fig. 20: Vertically integrated operational first guess error for 13 days with strong westerly flow over the Rocky Mountains in December 1990. Units N m^{-2}.